$K^-\,^3$He and K^+K^- interactions in the $pd \to {}^3\mathrm{He}\,K^+K^-$ reaction

V.Yu. Grishina
Institute for Nuclear Research, 60th October Anniversary Prospect 7A, 117312 Moscow, Russia

M. Büscher*
Institut für Kernphysik, Forschungszentrum Jülich, D-52425 Jülich, Germany

L.A. Kondratyuk
Institute of Theoretical and Experimental Physics, B. Cheremushkinskaya 25, 117218 Moscow, Russia

(Dated: February 4, 2008)

We investigate the $K^-\,^3$He and K^+K^- interactions in the reaction $pd \to {}^3\mathrm{He}K^+K^-$ near threshold and compare our model calculations with data from the MOMO experiment at COSY-Jülich. A large attractive effective K^-p amplitude would give a significant $K^-\,^3$He final-state interaction effect which is not supported by the experimental data. We also estimate upper limits for the $a_0(980)$ and $f_0(980)$ contributions to the produced K^+K^- pairs.

PACS numbers: 25.80.nv, 13.60.Le, 13.75.Jz, 25.10.+s,
Keywords: Nuclear reactions involving few nucleon systems; Hadron-induced low- and intermediate-energy reactions and scattering (≤ 10 GeV); K meson production; K^+K^- interaction; ϕ meson production

I. INTRODUCTION

Low energy $\bar{K}N$ and $\bar{K}A$ interactions have been subject of extensive studies during the last two decades. The well known phenomenological analysis of $\bar{K}N$ scattering lengths by Martin [1] demonstrated that the s-wave K^-p scattering length is large and repulsive, $\mathrm{Re}\,a(K^-p) = -0.67$ fm, while for the K^-n case it is moderately attractive, $\mathrm{Re}\,a(K^-n) = 0.37$ fm. Recently, new data on the strong-interaction $1s$ level shift of kaonic hydrogen atoms were obtained at KEK (KpX experiment) [2, 3] and Frascati (DEAR) [4]. They correspond to the following repulsive values of the K^-p scattering length

$$a(K^-p) = -(0.78 \pm 0.18) + i(0.49 \pm 0.37)\ \mathrm{fm} \qquad (1)$$

for KpX, and

$$\begin{aligned} a(K^-p) &= (-0.468 \pm 0.090_{\mathrm{stat}} \pm 0.015_{\mathrm{syst}}) \\ &+ i(0.302 \pm 0.135_{\mathrm{stat}} \pm 0.036_{\mathrm{syst}})\ \mathrm{fm} \end{aligned} \qquad (2)$$

for DEAR.

Nevertheless, as it was argued in Refs. [5, 6], the actual K^-p interaction can be attractive if the isoscalar $\Lambda(1405)$ resonance is a bound state of the $\bar{K}N$ system. Such a scenario can be explained within Chiral Perturbation Theory where the leading order term in the chiral expansion for the K^-N amplitude is attractive. Further developments in the analysis of the $\bar{K}N$ interaction based on chiral Lagrangians can be found in Refs. [7–11]. Such a peculiar behavior of the $\bar{K}N$ dynamics leads to very interesting in-medium effects for anti-kaons in finite nuclei as well as in dense nuclear matter, including neutron stars, see *e.g.* papers [12–17] and references therein.

Exotic few-body nuclear systems involving the $\bar{K}$-meson as a constituent were predicted by Akaishi and Yamazaki [18]. They argued that the $\bar{K}N$ interaction is characterized by a strong I=0 attraction, which allows the few-body systems to form dense and deeply bound $\bar{K}$-nuclear states.

Evidence for a strange tribaryon $S^0(3115)$ with a width below 21 MeV was observed in the interaction of stopped K^--mesons with ^{4}He [19]. This state was interpreted as a candidate for a deeply bound state $(\bar{K}NNN)^{Z=0}$ with I=1, I_3=−1 [19, 20]. However, the $S^0(3115)$ is about 100 MeV below the predicted mass, and in the experiment an isospin-1 state was detected at a position where no such peak was predicted. It was discussed in Ref. [20] that this discrepancy can be resolved by tuning parameters of the model [18]. The results of Akaishi and Yamazaki [18] were criticized by Oset and Toki [21] who argued that the model of Ref. [18] is unrealistic. Oset and Toki also suggested that the peaks in the reaction with ^{4}He can be due to K^- absorption on a pair of nucleons. This suggestion puts doubt whether a narrow tribaryon $S^0(3115)$ really exists.

Another tentative evidence for a K^-pp bound state produced in K^- absorption at rest on different nuclear targets was found by the FINUDA collaboration [22]. It was detected through its two-body decay into a Λ and a proton. The signal in the Λp invariant-mass distribution is about 115 MeV below the expected mass of the Λp system in case of non-bound K^-NN absorption. Magas *et al.* [23] showed that the FINUDA signal can also be explained by a $K^-pp \to \Lambda p$ reaction followed by final-state interactions (FSI) of the produced particles with the remnant nucleus.

Thus, it is obvious that further searches for bound kaonic nuclear states as well as new data on the interactions of $\bar{K}$-mesons with light nuclei are of great interest.

*Electronic address: m.buescher@fz-juelich.de

In a recent paper [24] we presented a first calculation of the s-wave $K^-\alpha$ scattering length $A(K^-\alpha)$ and discussed how to determine it from the $K^-\alpha$ invariant-mass distribution in the reaction $dd{\to}\alpha\, K^+K^-$ near threshold. In the present paper we consider the $K^-\,{}^3$He FSI in the reaction $pd \to {}^3\mathrm{He}\, K^+K^-$ and compare our calculations with the existing data on this reaction near threshold [25, 26]. We also analyze the K^+K^- relative-energy distribution for this reaction and estimate possible contributions from the $a_0(980)$ and $f_0(980)$ resonances.

Our paper is organized as follows: In Sect. II we calculate the $K^-\,{}^3$He and $K^-\alpha$ scattering lengths. In Sect. III an analysis of the $K^-\,{}^3$He FSI in the reaction $pd \to {}^3\mathrm{He}\, K^+K^-$ is presented. In Sect. IV we analyze the differential K^+K^- distributions and discuss the possible contributions from the $a_0/f_0(980) \to K^+K^-$ channels. Our conclusions are given in Sect. V.

II. $K^-\,{}^3$He AND $K^-\alpha$ SCATTERING LENGTHS

In order to calculate the s-wave $K^-\,{}^3$He and $K^-\alpha$ scattering lengths and corresponding enhancement factors we use the multiple-scattering approach (MSA) in the fixed center approximation described in detail in our previous paper [24]. For the nuclear density we use a factorized model with the single-nucleon density in Gaussian form

$$\rho(\mathbf{r}) = \frac{1}{(\pi\, R^2)^{3/2}}\ \mathrm{e}^{-r^2/R^2}\ , \qquad (3)$$

where $R^2/4 = 0.62$ and 0.7 fm^2 for ^{4}He and ^{3}He, respectively. Note, that the independent particle model gives a rather good description of the ^{4}He and ^{3}He electromagnetic form factors up to a momentum transfer $\mathbf{q}^2 = 8$ fm^{-2} (see *e.g.* Ref. [27]).

Some theoretical predictions for the $K^-\alpha$ and $K^-\,{}^3$He scattering lengths, $A(K^-\alpha)$ and $A(K^-\,{}^3\mathrm{He})$, have been published in Refs. [24, 28]. In Table I we present new results calculated for different $\bar{K}N$ inputs as compared to Refs. [24, 28]. We consider the $\bar{K}N$ scattering lengths from a K-matrix fit (Set 1) [29] as well as the predictions for the $\bar{K}N$ scattering amplitudes based on the chiral unitary approach of Ref. [9] (Set 2). The constant scattering-length fit from Conboy [30] is denoted as Set 3. We note that the $\bar{K}N$ scattering lengths described by Sets 1–3 correspond to their vacuum values. At the same time Sets 4–5 describe the effective $\bar{K}N$ scattering lengths that contain in-medium effects.

One of the most extensive analyses of the effective $\bar{K}N$ interactions in nuclear medium has been presented by Ramos and Oset [31] within a self-consistent microscopic theory. The resulting K^- attraction in medium has been found to be smaller than predicted by other theories and approximation schemes. The isospin-averaged effective $\bar{K}N$ scattering length is moderately attractive and its real part does not exceed the value of

$$\mathrm{Re}\ a^{\mathrm{eff}} \simeq 0.3\,\mathrm{fm}\ , \qquad (4)$$

at nuclear density $\rho \geq 0.3\rho_0$. The obtained shallow K^--nucleus optical potential with a depth of -50 MeV (for the real part of the potential at $\rho = \rho_0$) was successfully used to reproduce the experimental shifts and widths of kaonic atoms over the periodic table [32].

In contrast to the results of Ref. [31], Akaishi and Yamazaki [18] proposed much more attractive optical potential which corresponds to the following effective $\bar{K}N$ scattering lengths for the $I = 0, 1$ channels in the nuclear medium

$$\begin{aligned} a_0^{\mathrm{eff}} &= 2.9 + i1.1\,\mathrm{fm}\ , \\ a_1^{\mathrm{eff}} &= 0.43 + i0.30\,\mathrm{fm}\ . \end{aligned} \qquad (5)$$

According to the Akaishi and Yamazaki approach, such a strong attraction appears already in the case of few-nucleon systems generating deeply bound $\bar{K}$-nuclear states [18].

In order to demonstrate the sensitivity of our results to possible modifications of the $\bar{K}N$ scattering amplitudes in the presence of nuclei we consider as Set 4 the moderately attractive effective scattering length from Ref. [31]. As Set 5 we choose the strongly attractive in-medium solution found in Refs. [18, 20] and given by Eq.(5).

The calculated values of the $A(K^-\alpha)$ and $A(K^-\,{}^3\mathrm{He})$ within the multiple-scattering theory are listed in the 5^{th} and 6^{th} columns of Table I. They are very similar for Sets 1 and 2, $A^{\mathrm{MS}}(K^-\alpha) \sim (-1.9 + i1.0)$ fm and $A^{\mathrm{MS}}(K^-\,{}^3\mathrm{He}) \sim (-1.6 + i1.0)$ fm. The results for Set 3 are quite different especially for the imaginary part of $A^{\mathrm{MS}}(K^-\,{}^3\mathrm{He})$ and the real part of $A^{\mathrm{MS}}(K^-\alpha)$. The calculations with the effective $\bar{K}N$ amplitude from Ref. [31] give the $K^-\alpha$ scattering length with an imaginary part roughly two times larger than the result obtained with the vacuum $\bar{K}N$ scattering lengths. Not surprisingly, the exotic Set 5 for the elementary amplitudes extracted from Refs. [18, 20] leads to enormously large scattering lengths for $K^-\alpha$ and $K^-\,{}^3$He systems with real parts of -3.5 fm and -4 fm, respectively. In the case of the Set 5 we also performed calculations using the single-nucleon density parameters in Eq. (3) from Ref. [18] $R^2/4 = 0.48$ fm^2 and 0.64 fm^2 for ^{4}He and ^{3}He, respectively. The corresponding results, presented in square brackets in Table I, show a not very high sensitivity to the parameter R.

Alternatively we considered the optical potential

$$V^{\mathrm{opt}}_{K^-A}(\mathbf{r}) = -\frac{2\,\pi}{\mu_{\bar{K}N}}\ \left[a_{K^-p}\, Z\rho_p(r) + a_{K^-n} N\rho_n(r)\right]\ , \qquad (6)$$

where $\mu_{\bar{K}N}$ is the reduced mass of the $\bar{K}N$ system and $\rho_p(r) = \rho_n(r) = \rho(r)$ is defined by Eq. (3) with eliminated c.m. motion, i.e. $R^2 \to R^2\ (A-1)/A$. The results for $A(K^-\alpha)$ are presented in the last column of the Table I. $A^{\mathrm{opt}}(K^-\alpha)$ was found to be about 30–40% smaller than $A^{\mathrm{MS}}(K^-\alpha)$ for the vacuum parameters of the $\bar{K}N$ interactions. In the case of Set 5 the $K^-\alpha$ scattering length was calculated using the optical-potential model with $R^2/4 = 0.62$ fm^2 or $R^2/4 = 0.48$ fm^2 (the latter solution is presented in square brackets). This result is

TABLE I: $K^-\alpha$ and $K^-\,{}^3$He scattering lengths obtained within the multiple-scattering approach and $K^-\alpha$ scattering length calculated using the optical-potential model for various choices of the elementary $\bar{K}N$ scattering lengths $a_I(\bar{K}N)$ $(I = 0, 1)$. The effective $\bar{K}N$ scattering length of Set 4 is extracted from the isospin averaged optical potential. Therefore it can only be applied for the calculation of $A(K^-\alpha)$.

Set	Ref.	$a_0(\bar{K}N)$ [fm]	$a_1(\bar{K}N)$ [fm]	$A^{\rm MS}(K^-\alpha)$ [fm]	$A^{\rm MS}(K^-{}^3{\rm He})$ [fm]	$A^{\rm opt}(K^-\alpha)$ [fm]
1	[29]	$-1.59 + i0.76$	$0.26 + i0.57$	$-1.80 + i0.90$	$-1.50 + i0.83$	$-1.26 + i0.60$
2	[9]	$-1.31 + i1.24$	$0.26 + i0.66$	$-1.98 + i1.08$	$-1.66 + i1.10$	$-1.39 + i0.65$
3	[30]	$-1.03 + i0.95$	$0.94 + i0.72$	$-2.24 + i1.58$	$-1.52 + i1.80$	$-1.59 + i0.88$
4	[31]	$0.33 + i0.45$ isospin average		$-1.47 + i2.22$		$-1.51 + i1.20$
5	[18]	$2.9 + i1.1$	$0.43 + i0.30$	$-3.49 + i1.80$	$-3.93 + i4.03$	$-1.57 + i0.74$
				$[-2.99 + i1.27]$	$[-3.91 + i3.62]$	$[-1.31 + i0.73]$

more than a factor of two smaller as compared to the solution for Set 5 obtained in the framework of the MSA.

The single-scattering term of the total K^-A scattering length is the same in both the muliple-scattering and optical-potential schemes. It is equal to

$$A^{(1)}(K^-A) = \frac{\mu_{\bar{K}A}}{\mu_{\bar{K}N}}\,(N a_{\bar{K}n} + Z a_{\bar{K}p})\ ,$$

where $\mu_{\bar{K}A}$ is the K^-A reduced mass. Note that in the case of the K^-d system the higher order rescattering corrections were analyzed within the fixed center approximation to the Faddeev equations with the input parameters from the chiral unitary approach [33]. Their contributions were evaluated and found to be very noticeable. Within the optical-potential model the next-to-leading order scattering terms $A^{(n)}(K^-A)$ are defined using different averaging procedures over the coordinates of the nucleons than in the case of the MSA in the fixed center approximation. However the total meson-nucleus scattering length obtained within the simplest optical-potential model needs some corrections especially important for the few-body systems. Particularly, in Ref. [34] the isospin-symmetric case of the η-nucleus system was considered with equal elementary scattering amplitudes of the η meson on the proton and neutron. For the η-nucleus scattering length calculated using the optical-potential model it was suggested that each multiple-scattering term of n-th order should be corrected with q factor $((A-1)/A)^n$ to remove multiple collisions on the same nucleon. Such a correction cannot be used for the K^-A optical-potential calculations due to the significantly different K^-n and K^-p scattering lengths. The advantage of the MSA applied to the K^-A system is that it explicitly takes into account the difference between the elementary K^-p and K^-n scattering amplitudes (see Ref. [24]). Furthermore, if the $\bar{K}N$ interaction radius is small as compared to the size of the nucleus, the MSA is valid and the overall scattering amplitude can be expressed in terms of the individual on-shell meson-nucleon amplitudes without extra free parameters. The $\bar{K}N$ potential constructed by Akaishi and Yamazaki is of short range type with $R = 0.66$ fm (see Ref. [18]). Using this assumption we can reliably apply the MSA for the description of the K^--light nucleus system.

III. $K^-\,{}^3$He FSI IN $pd\to{}^3$He K^+K^-

We now discuss the $K^-\,{}^3$He FSI effect in the reaction $pd \to {}^3{\rm He}\,K^+K^-$ near threshold and compare our calculations performed in the MSA with the data from the MOMO experiment [25, 26] at COSY-Jülich. The MOMO collaboration measured at three different beam energies, corresponding to excess energies of $Q = 35,\ 41$ and 55 MeV with respect to the K^+K^- threshold. We only consider the data at the central energy since these constitute the best compromise between available phase space and resolution for our analyses. The MOMO data are presented in terms of relative energies $T_{K^-\,{}^3{\rm He}}$ and $T_{K^+K^-}$; in the non-relativistic approximation they can be expressed through the corresponding invariant masses M_{ij} by $T_{ij} = M_{ij} - m_i - m_j$. Since the MOMO experiment was not sensitive to the charge of the detected kaons, the measured $T(K,\,{}^3{\rm He})$ distributions (see Fig. 1) are symmetric with respect to $Q/2$. This is taken into account in our calculations by constructing the half-sum of the K^+ and K^- contributions.

As the first step of our analysis we neglect all FSI effects and investigate the contribution of the $\phi(1020)$ meson by fitting the K^+K^- relative-energy distribution (taking into account the experimental mass resolution quoted in Ref. [26]). The ϕ-meson contribution is found to be about 16% of the total cross section (9.6 ± 1.0) nb, which is in agreement with the result from Ref. [26]. In Fig. 1 we show the K^+K^- relative-energy distribution; the solid line describes the incoherent sum of a pure phase-space distribution and the $\phi(1020)$ contribution.

The short-dashed and dashed lines in Fig. 1 show the influence of the $K^-\,{}^3$He FSI on the K^+K^- relative-energy distribution. The dash-dotted line shows the effect for the strongly modified $\bar{K}N$ scattering lengths in nuclear medium (Set 5) leading to the deeply bound states.

In Fig. 1 we also present calculations of the $K\,{}^3$He relative-energy spectrum. The predictions are normalized to the total $pd \to {}^3{\rm He}\,K^+K^-$ cross section of 9.6 nb. The dash-dotted line, corresponding to Set 5, demonstrates a pronounced deformation of the $K\,{}^3$He relative-energy spectrum in the region of small energies. It is in clear contradiction to the data.

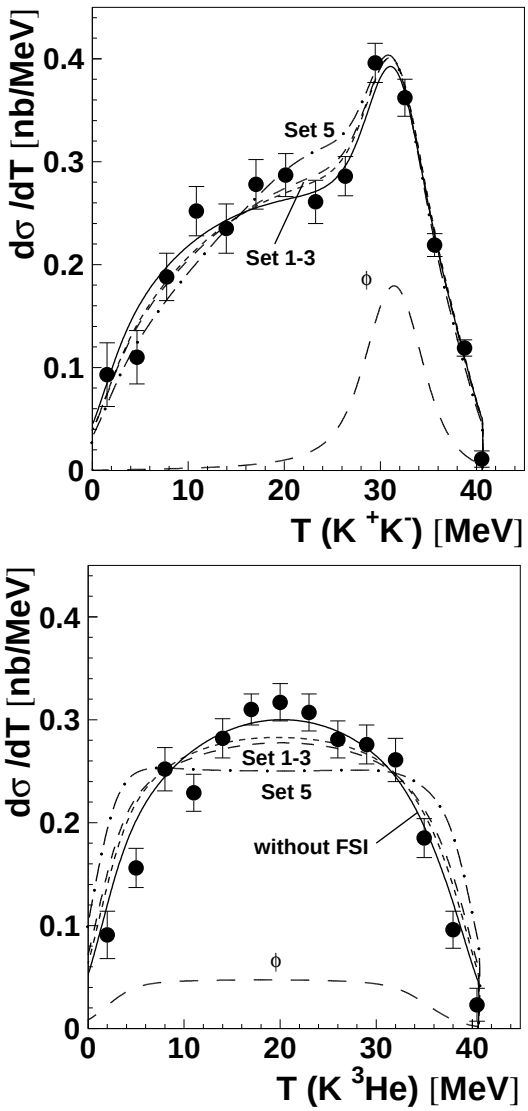

FIG. 1: Distribution of the K^+K^- (upper) and $K\,^3$He (lower) relative energies for the $pd \to {}^3\mathrm{He}\,K^+K^-$ reaction at an excess energy of 41 MeV. The MOMO data are taken from Refs. [25, 26]. The solid line describes the incoherent sum of a pure phase-space distribution and the $\phi(1020)$ contribution (long-dashed line). The short-dashed and dashed lines show the effect of the $K^-\,^3$He FSI for parameters of Set 1 and 3, respectively. The dash-dotted line shows the effect for the strongly modified $\bar{K}N$ scattering lengths in nuclear medium [18] leading to the deeply bound states.

While the solution without FSI is in best agreement with the data, the results with $K^-\,^3$He FSI calculated using elementary $\bar{K}N$ amplitudes from Sets 1–3 cannot be ruled out due to the uncertainties of the MSA (see *e.g.* Ref. [24]) and the experimental errors.

IV. K^+K^- ENERGY SPECTRUM AND $a_0(980)/f_0(980)$ PRODUCTION

The a_0 and f_0 resonances may give some contributions to the $pd \to {}^3\mathrm{He}\,K^+K^-$ cross section. In this case one can write the invariant K^+K^- mass distribution as

$$\frac{\mathrm{d}\sigma_{pd\to{}^3\mathrm{He}\,K^+K^-}}{\mathrm{d}M} = \frac{\mathrm{d}\sigma_{\mathrm{BG}}}{\mathrm{d}M} + \frac{\mathrm{d}\sigma_{\phi}}{\mathrm{d}M} + \frac{\mathrm{d}\sigma_{a_0}}{\mathrm{d}M} + \frac{\mathrm{d}\sigma_{f_0}}{\mathrm{d}M}\ . \quad (7)$$

The first term describes the non-resonant K^+K^- production with a constant interaction amplitude near threshold. The $K^-\,^3$He FSI effects can be neglected since their influence on the K^+K^- distribution is very small, see Fig. 1. The $\phi(1020)$-meson contribution $\mathrm{d}\sigma_\phi/\mathrm{d}M$ has already been considered in the previous section. The last two terms reflect the contributions from the $a_0(980)$ and $f_0(980)$ resonances. Each of them can be written as a product of the total a_0- or f_0-production cross section σ_{a_0} (σ_{f_0}) as a function of the "running" mass M and the Flatté mass distribution. For example, in case of a_0 production we have

$$\frac{\mathrm{d}\sigma_{a_0K^+K^-}}{\mathrm{d}M^2}(s,M) = \sigma_{a_0}(s,M) \times C_{\mathrm{F}}\frac{M_R\Gamma_{a_0K^+K^-}(M)}{(M^2-M_R^2)^2+M_R^2\Gamma_{\mathrm{tot}}^2(M)} \quad (8)$$

with the total width $\Gamma_{\mathrm{tot}}(M) = \Gamma_{a_0K\bar{K}}(M) + \Gamma_{a_0\pi\eta}(M)$ and $\Gamma_{a_0K^+K^-}(M) = 0.5\,\Gamma_{a_0K\bar{K}}$. The constant C_{F} is introduced to normalize the total decay probability of the a_0 to unity. The partial widths

$$\begin{aligned}\Gamma_{a_0K\bar{K}}(M) &= g^2_{a_0K\bar{K}}\frac{q_{K\bar{K}}}{8\pi M^2},\\ \Gamma_{a_0\pi\eta}(M) &= g^2_{a_0\pi\eta}\frac{q_{\pi\eta}}{8\pi M^2}\end{aligned} \quad (9)$$

are proportional to the decay momenta in the c.m. system

$$\begin{aligned}q_{K\bar{K}} &= \frac{\left[(M^2-(m_K+m_{\bar{K}})^2)(M^2-(m_K-m_{\bar{K}})^2)\right]^{1/2}}{2M}\\ q_{\pi\eta} &= \frac{\left[(M^2-(m_\pi+m_\eta)^2)(M^2-(m_\pi-m_\eta)^2)\right]^{1/2}}{2M}\ ,\end{aligned}$$

for a particle of mass M decaying to $K\bar{K}$ and $\pi\eta$, respectively. The contribution of the f_0-meson can be written in a similar manner taking into account its decays into $\pi\pi$ and $K\bar{K}$. The parameters $g_{a_0\pi\eta}$, $R_{a_0} = g^2_{a_0K\bar{K}}/g^2_{a_0\pi\eta}$, M_R and $g_{f_0\pi\pi}$, $R_{f_0} = g^2_{f_0K\bar{K}}/g^2_{f_0\pi\pi}$, M_R of the Flatté amplitudes for the a_0 and f_0 resonances can be taken from literature (see *e.g.* most recent papers [35–37] and references therein).

Using Eq. (7) we calculate the K^+K^- mass distributions with parameters of Set a_0[Crystal Barrel] [38] and Set a_0[E852] [39] for the $a_0(980)$ resonance contribution as well as Set f_0[BES][40] and Set f_0[E791][41] for the $f_0(980)$. These parameters are presented in Table II.

TABLE II: Flatté parameters for the $a_0(980)$ and $f_0(980)$ resonances.

Set	Ref.	$g_{a_0\pi\eta}$ or $g_{f_0\pi\pi}$ [GeV]	R_{a_0} or R_{f_0} [GeV]	M_R
a_0[CB]	[38]	2.3	1.03	0.999
a_0[E852]	[39]	2.47	0.91	1.001
f_0[BES]	[40]	1.17	17.72	0.965
f_0[E791]	[41]	1.04	0.22	0.977

We then compare the shape of the calculated spectra with that of the measured $T(K^+K^-)$ distribution. The solution without a_0 and f_0 resonances is in best agreement with the data with $\chi^2_{\rm min} = 11.5$. The different curves in Fig. 2 represent the relative contributions of the $a_0(980)$ or $f_0(980)$ meson versus the fraction of the $\phi(1020)$ meson obtained at $\chi^2 = \chi^2_{\rm min}+1, \chi^2_{\rm min}+2$ and $\chi^2_{\rm min}+3$. It is seen that the $a_0(980)$ contribution might reach 20–25% within a $\chi^2_{\rm min}+3$ limit while that from the f_0 does not exceed $\sim 10\%$ of the total $pd \to {}^3{\rm He}\,K^+K^-$ cross section at $Q = 41$ MeV.

To describe the MOMO data we just added the differential cross sections for the various channels, neglecting possible interference between the a_0-, f_0- and non-resonant contributions to the full $pd \to {}^3{\rm He}\,K^+K^-$ amplitude. There is no simple way to calculate interference terms that depend on the spin structure and relative phases of different amplitudes. Therefore, using the K^+K^- relative-energy spectrum one can only obtain qualitative estimates of the a_0 and f_0 resonance contributions. Nevertheless we conclude that in the $pd \to {}^3{\rm He}\,K^+K^-$ reaction near the threshold the K^+K^- pairs are mainly produced non-resonantly.

V. CONCLUSIONS

We present predictions for the $K^-\,{}^3$He and $K^-\alpha$ scattering lengths obtained within the framework of the multiple-scattering approach. We have studied uncertainties of the calculations due to the presently available elementary $\bar{K}N$ scattering lengths. We have compared the results for $A(K^-\alpha)$ with values obtained using the optical-potential model. We have also considered the $K^-\,{}^3$He and K^+K^- final-state interactions in the reaction $pd \to {}^3{\rm He}\,K^+K^-$ near threshold and compare our model calculations with the existing data from the MOMO collaboration [25, 26]. We find that a strongly modified $\bar{K}N$-effective scattering length extracted from the very attractive K^-A potential proposed by Akaishi and Yamazaki [18] might lead to a pronounced deformations of the $K^-\,{}^3$He and K^+K^- relative-energy spectra which are in contradiction to the data. We also derive upper limits on the $a_0(980)$- and $f_0(980)$-production rates and find them to be on a level of about 25% for the a_0 and 10% for the f_0 at an excess energy of 41 MeV.

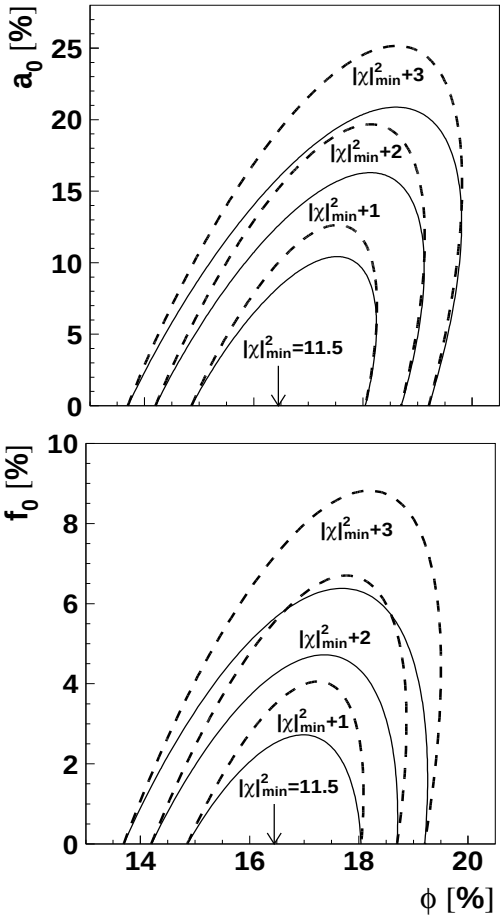

FIG. 2: Result of our fit to the experimental K^+K^- mass distribution for the $pd \to {}^3{\rm He}\,K^+K^-$ reaction at an excess energy of 41 MeV. The $\chi^2 = \chi^2_{\rm min}+1, \chi^2_{\rm min}+2, \chi^2_{\rm min}+3$ contour lines are obtained for relative contributions of $a_0(980)$ or $f_0(980)$ as a function of the $\phi(1020)$-meson fraction. In the upper figure the solid and dashed lines were calculated using the Flatté distributions for the a_0 meson with the parameters of Set a_0[Crystal Barrel] and Set a_0[E852], respectively. In the lower figure the solid and dashed contour lines correspond to the contribution of the f_0 meson with the Flatté parameters of Set f_0[BES] and Set f_0[E791].

VI. ACKNOWLEDGMENTS

We are grateful to Hartmut Machner, Hans Ströher and Colin Wilkin for fruitful discussions. This work was supported by DFG grant 436 RUS 113/787 and RFBR grant 06-02-04013 and the Russian Federal Agency of Atomic Energy. V.G. acknowledges support by the COSY FFE grant No. 41520739 (COSY-071).

[1] A.D. Martin, Nucl. Phys. B **179**, 33 (1981).
[2] T.M. Ito *et al.*, Phys. Rev. C **58**, 2366 (1998).
[3] M. Iwasaki *et al.*, Phys. Rev. Lett. **78**, 3067 (1997).
[4] C. Guaraldo *et al.*, Eur. Phys. J. A **19**, 185 (2004); G. Beer *et al.*, Phys. Rev. Lett. **94**, 212302 (2005).
[5] R. H. Dalitz, T. C. Wong, G. Rajasekaran, Phys. Rev. **153**, 1617 (1967).
[6] P. B. Siegel, W. Weise, Phys. Rev. C **38**, 2221 (1988).
[7] T. Waas, N. Kaiser, W.Weise, Phys. Lett. B **365**, 12 (1996); Phys. Lett. B **379** (1996) 34; W. Weise, Nucl. Phys. A **610**, 35 (1996).
[8] E. Oset, A. Ramos, Nucl. Phys. A **635**, 99 (1998).
[9] J.A. Oller, U.-G. Meißner, Phys. Lett. B **500**, 263 (2001).
[10] M. Lutz, E.E. Kolomeitsev, Nucl.Phys. A **700**, 193 (2002).
[11] J.A. Oller, J. Prades, M. Verbeni, Phys. Rev. Lett. **95**, 172502 (2005).
[12] A. Sibirtsev, W. Cassing, Nucl. Phys. A **641**, 476 (1998).
[13] M. Lutz, Phys. Lett. B **426**, 12 (1998).
[14] A. Sibirtsev, W. Cassing, Phys. Rev. C **61**, 057601 (2000).
[15] A. Ramos, S. Hirenzaki, S.S. Kamalov, T.T.S. Kuo, Y. Okumura, E. Oset, A. Polls, H. Toki, L. Tolos, Nucl. Phys. A **691**, 258c (2001).
[16] H. Heiselberg, M. Hjorts-Jensen, Phys. Rep. **328**, 237 (2000).
[17] A. Cieply, E. Fridman, A. Gal, J. Mares, Nucl. Phys. A **696**, 173 (2001).
[18] Y. Akaishi and T. Yamazaki, Phys. Rev. C **65**, 044005 (2002).
[19] T. Suzuki, *et al.*, Phys. Lett. B **597**, 263 (2004); M. Iwasaki *et al.*, arXiv:nucl-ex/0310018.
[20] Y. Akaishi, A. Dote, T. Yamazaki, Phys. Lett. B **613**, 140 (2005).
[21] E. Oset, H. Toki, Phys. Rev. C **74**, 015207 (2006).
[22] M. Agnello *et al.*, Phys. Rev. Lett. **94**, 212303 (2005).
[23] V. K. Magas, E. Oset, A. Ramos, H. Toki, Phys. Rev. C **74**, 025206 (2006).
[24] V.Yu. Grishina, L.A. Kondratyuk, A. Sibirtsev, M. Büscher, S. Krewald, U.-G. Meißner, F.P. Sassen, Eur. Phys. J. A **25**, 159 (2005).
[25] H.A. Schnitker, *"Zwei-Kaonen-Produktion nahe der Schwelle in der Reaktion* $pd \to {}^3He\,K^+K^-$ *mit dem Experiment MOMO an COSY"* (Dissertation Universität Bonn 2002).
[26] F. Bellemann *et al.*, *Phys. Rev. C, in print*, arXiv:nucl-ex/0608047.
[27] V.N. Boitsov, L.A. Kondratyuk, V.B. Kopeliovich, Sov. J. Nucl. Phys. **16**, 287 (1973).
[28] L. Kondratyuk, V. Grishina, M. Büscher, 6^{th} Int. Conf. on Nuclear Physics at Storage Rings (STORI2005), Bonn, Germany, 23–26 May 2005; Schriften des Forschungszentrums Jülich, Matter and Materials, vol. **30**, 2006, ISSN 1433-5506, p. 165 [arXiv:nucl-th/0507021].
[29] R. C. Barrett, A. Deloff, Phys. Rev. C **60**, 025201 (1999).
[30] J.E. Conboy, Rutherford-Appleton Lab. Report, RAL-85-091 (1985).
[31] A. Ramos, E. Oset, Nucl. Phys. A **671**, 481 (2000).
[32] S. Hirenzaki, Y. Okumura, H. Toki, E. Oset, A. Ramos, Phys. Rev. C **61**, 055205 (2000).
[33] S.S. Kamalov, E. Oset, A. Ramos, Nucl. Phys. A **690**, 494 (2001).
[34] S. Wycech, A.M. Green, J.A. Niskanen, Phys. Rev. C **52**, 544 (1995).
[35] N.N. Achasov, A.N. Kiselev, Phys. Rev. D **68**, 014006 (2003).
[36] V.V. Anisovich, Phys. Usp.**47**, 45 (2004) [Usp. Fiz. Nauk **47**, 49 (2004)].
[37] V. Baru, J. Haidenbauer, C. Hanhart, A.E. Kudryavtsev, U.-G. Meißner, Eur. Phys. J. A **23**, 523 (2005).
[38] A. Abele *et al.*, Phys. Rev. D **57**, 3860 (1998).
[39] S. Teige *et al.*, Phys. Rev. D **59**, 012001 (2001).
[40] M. Ablikim *et al.*, Phys. Lett. B **607**, 243 (2005).
[41] M. Aitala *et al.*, Phys. Rev. Lett.**86**, 765 (2001).